

## Eliminating Segregation in Free-Surface Flows of Particles

Deliang Shi, Adetola A. Abatan, Watson L. Vargas, and J. J. McCarthy\*

*Department of Chemical and Petroleum Engineering University of Pittsburgh Pittsburgh, Pennsylvania 15261, USA*  
(Received 21 February 2007; revised manuscript received 13 July 2007; published 4 October 2007)

By introducing periodic flow inversions, we show both experimentally and computationally that forcing with a value above a critical frequency can effectively eliminate both density and size segregation. The critical frequency is related to the inverse of the characteristic time of segregation and is shown to scale with the shear rate of the particle flow. This observation could lead to new designs for a vast array of particle processing applications and suggests a new way for researchers to think about segregation problems.

DOI: [10.1103/PhysRevLett.99.148001](https://doi.org/10.1103/PhysRevLett.99.148001)

PACS numbers: 45.70.Mg

Particle segregation has been a topic of intense research and industrial frustration for many decades [1–4]. When particles differ in almost any mechanical property, processing typically leads to pattern formation [5,6], layering [7,8], or complete separation of the materials [9–11] and this nonhomogeneity can cause dramatic revenue loss and product failure in a variety of industries. In particular, particles of different size and density may segregate quite strongly in free-surface flows; the larger (lighter) particles often rise to the top, while the smaller (denser) particles sink to the bottom. While recent efforts have made inroads in controlling segregation using cohesion [12,13] or particle modification (to *balance* competing segregation modes) [14,15], even these laudable efforts are not robust to changes in particle properties and/or cohesion degree and therefore are applicable to only a subset of typical industrial practice. Here, we show that periodic flow inversions either manually (in a chute) or via selective baffle placement (in a tumbler-type mixer) can serve as a general method for eliminating segregation in free-surface flows, perhaps the most common and well-studied of granular flows [16–18].

Time-modulation in fluid mixing and other dynamical systems [19] is a common practice, but has found only limited application in granular processing [20–22]. The key to adapting this idea to free-surface segregation lies in recognizing that it takes a finite time for material to segregate and that there is always a preferred direction that particles tend to segregate. In order to exploit these two facts, one needs to perturb the flow at a sufficiently high frequency,  $f$ , such that  $f > t_s^{-1}$ , where  $t_s$  is the characteristic segregation time.

A critical issue with this technique is that a full understanding of segregation kinetics—and therefore the characteristic segregation time,  $t_s$ —is still lacking. Nevertheless, using existing theoretical tools [9,23], an estimate of the value of  $t_s$ , and therefore the critical forcing frequency,  $f_{\text{crit}}$ , may be obtained via a scaling argument, as follows. One may write a segregation flux expression as  $J_s = v_s \phi$ , where  $v_s$  is the segregation velocity and  $\phi$  is the concentration of the segregating species. Taking density segregation as an example (size segregation is similar,

albeit more complex [23]), the segregation velocity will take the form  $v_s = K_s(1 - \bar{\rho})$  [9], where  $(1 - \bar{\rho})$  is the dimensionless density difference and  $K_s$  will depend on the local void fraction and granular temperature. The characteristic segregation time may then be written as  $t_s = R/[K_s(1 - \bar{\rho})]$ , where  $R$  is the radius of the particles. Using this value, we can define a segregation-based Péclet number as  $\text{Pe} = \frac{K_s(1 - \bar{\rho})R}{D}$ , where  $D$  is the collisional diffusivity. Because of the current theoretical uncertainty and the time-varying nature of our flow (as well as our granular temperature, etc.), we treat  $\beta = K_s R/D$  as a fitting parameter that should be a decreasing function of the fluctuation energy of the flow and should be close to unity at small to moderate energies [9]. This yields  $\text{Pe} = \beta(1 - \bar{\rho})$ , so that by using the diffusivity as given by Ref. [24] ( $D = 0.01R^2\dot{\gamma}$ ), we get  $t_s$  written as  $t_s = \frac{L\mu}{\text{Pe}} = \frac{R^2}{D\text{Pe}} = \frac{100}{\beta\dot{\gamma}(1 - \bar{\rho})}$ , where  $\dot{\gamma}$  is the shear rate. This suggests that the critical perturbation frequency,  $f_{\text{crit}}$ , will vary linearly with the shear rate as

$$f_{\text{crit}} = 0.01\beta\dot{\gamma}(1 - \bar{\rho}). \quad (1)$$

A simple geometry can be used to illustrate how this might be exploited. Consider a chute flow that “zigzags” periodically in such a way that, at each bend, the bottom of the previous flow leg now becomes the top of the next flow leg, and so on [see Fig. 1(a)]. If the length,  $L$ , of each leg is chosen such that  $L < U_{\text{avg}}t_s$  our theoretical arguments suggest that segregation can be effectively thwarted. While this thought experiment is theoretically satisfying, physically implementing this model system, either computationally or experimentally, is cumbersome. Instead, we examine two analogues of the zigzag mixer that are schematically depicted in Figs. 1(b) and 1(c).

Computationally, we mimic the zigzag mixer using a vertically bounded, periodic box whose sense of gravity oscillates vertically [see Fig. 1(b)]. Computations are based on the discrete element method [25,26] (DEM; for details, see Ref. [27]). The results of a number of zigzag simulations of density segregation are shown in Fig. 2 (right). In these 3D simulations, particles are initially randomly mixed, gravity is inclined at angles ranging

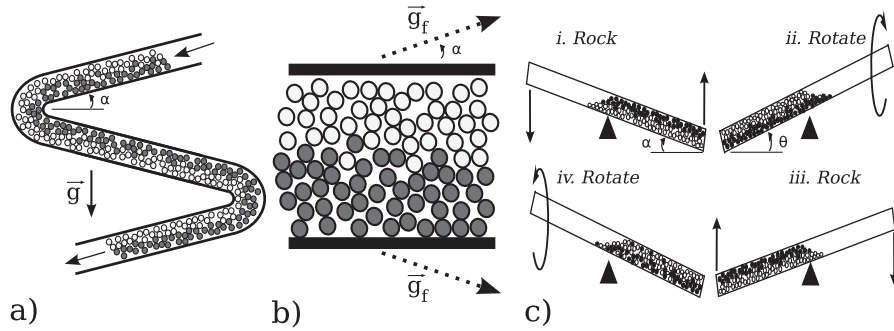


FIG. 1. A schematic representation of the (a) zigzag chute thought experiment, along with the (b) model simulation and (c) experiment used to approximate it. (a) In a vertical gravity field, the chute changes direction periodically so that the material becomes roughly inverted. (b) In our simulations, we use a simple model of this whereby the system is periodic in the flow direction and the inclined gravitational field,  $\vec{g}_f$ , has an oscillatory  $y$  component. (c) Experimentally, in order to achieve an asymptotic concentration distribution in a modest-size system we put particles in a square tube which is first rocked, then rotated in order to alter the sense of gravity [taking advantage of particles' tendency to behave like a solid during the rotate step by angling the tube at  $\theta \gg \alpha$  (repose angle) during the rotate step].

from  $22^\circ$ – $29^\circ$  with respect to the horizontal, and particle-roughened walls are used. Two particle bed heights, 10 and 20 particle diameters (2 mm), are examined as are two density ratios,  $\bar{\rho} = 0.5$  and  $0.25$  ( $\rho_{\text{light}} = 1000 \text{ kg/m}^2$ ). Using Eq. (1) with an empirically fit  $\beta = 0.1$  (due to high fluctuational energy within the flow), we plot the results of our simulations as a function of the ratio of the gravitational “flipping” frequency to  $f_{\text{crit}}$ . Here, the intensity of segregation (IS) [20] is a measure of the mixedness, where high values (typically greater than 0.25) imply poorly mixed systems while low values correspond to good mixing. This implies that the plot of our simulation results in Fig. 2 (right) should yield points with high values of IS for  $f/f_{\text{crit}} < 1$  and low values of IS when  $f/f_{\text{crit}} > 1$ . Despite the fact that many of our simulations resulted in nonlinear shear profiles—making appropriate values of  $\dot{\gamma}$  problematic—our results follow this trend to a remarkable extent when we obtain  $\dot{\gamma}$  from the most highly shearing portion of the flow.

Our experimental analogue of the zigzag mixer consists of hollow square rods (which allow a flow height of  $H = 1.8 \text{ cm}$ ) with lengths varying from 25 to 205 cm that are partially filled with (initially mixed) particles. In order to mimic the behavior of the zigzag mixer the rods are first rocked to induce flow down the inclined plane, and then rotated to change the orientation of the particles prior to the next rocking event [see Fig. 1(c)]. This process is repeated until the particle distribution no longer changes with time. Note that the rotate step is performed with the rod held at an angle ( $\theta$ ) significantly larger than the particles' angle of repose ( $\alpha$ ) so that no particle rearrangement occurs during the rotation. The rods are roughened on top and bottom to minimize particle slip and have their back (conductive) wall grounded to reduce electrostatic effects. Interestingly, in analyzing the results of these experiments, one notes that the ratio of  $f/f_{\text{crit}}$  is a function of the density ratio and aspect ratio of the tube only. This can be understood as follows. We first experimentally verified that the flow down

the tube is essentially linear (see Ref. [28]) so that  $\dot{\gamma} = 2U_{\text{avg}}/H$ , where  $U_{\text{avg}}$  is the average streamwise flow velocity and  $H$  is the height perpendicular to the flow direction. We then note that the effective forcing frequency is given as  $f = 2U_{\text{avg}}/L$ , so that [using Eq. (1)]

$$\frac{f}{f_{\text{crit}}} = \frac{100H}{\beta L(1 - \bar{\rho})}. \quad (2)$$

Taking  $\beta = 1.06$  (due to relatively low flow energy obtained during such a short acceleration), we plot the results of experiments with mixtures of glass acetate, acetate steel, and glass steel in Fig. 2 (left). The experiments are analyzed via image thresholding techniques to extract concentration profiles and IS values. For this plot, we define an experiment as yielding a mixed result if the IS value of the rocked-and-rotated particles is smaller than

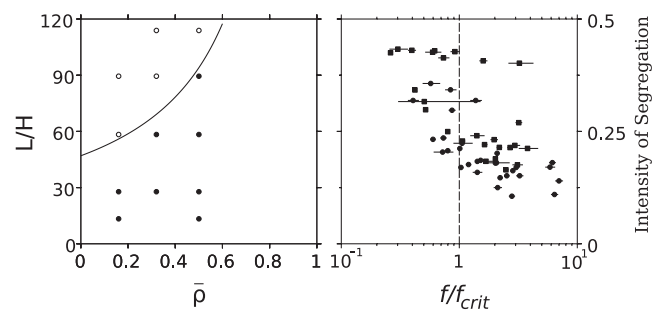


FIG. 2. Results from our models of the zigzag chute. (Left) Plotting our experimental results as a function of tube aspect ratio versus density ratio, we obtain agreement with theory for three different density ratios. Here the line is a plot of Eq. (2) with  $\beta = 1.06$ , the solid circles denote mixed systems, and the open circles denote segregated systems. (Right) Under a wide range of conditions, our computational results show high (low) values of IS when  $f/f_{\text{crit}}$  is less (greater) than 1. The closed circles denote simulations using a density ratio of 0.25, while the squares represent 0.5. Lines through the points show the standard deviation of the shear rate calculation.

that of a control experiment where the rotate step is omitted, otherwise it is denoted as a segregated result. In this way, we eliminate the impact of rod length on our evaluation of mixing.

Turning toward a practical application of this observation we recognize that, industrially, baffles are often used to augment mixing; however, we will show that baffles attached at the periphery of a tumbler are ineffective in reducing segregation. This can be understood by tracking the preferred direction of segregation within these drums, whereby one notes that the static portion of the bed simply “stores” the material and returns it in almost the same orientation for its next pass through the surface layer (i.e., it undergoes a full  $180^\circ$  change in orientation prior to returning to the flowing layer; see Fig. 3). This results in asymptotically segregated systems even for drums whose surface length,  $L$ , is small compared to  $U_{\text{mean}}t_s$ . If we instead place baffles near the axis of rotation, we periodically alter the flowing layer so that we achieve both (a) a smaller average uninterrupted flow length,  $L$ , and (b) periodic variations in the effective direction of segre-

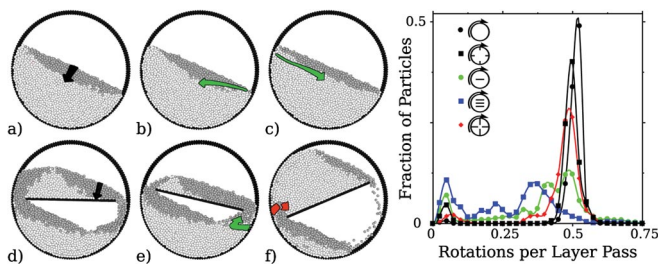


FIG. 3 (color). Images (a)–(f) show particle positions from DEM simulations for an unbaffled tumbler (a)–(c) and a tumbler with a single axially-located baffle (d)–(f). The light colored particles are in the fixed bed portion of the flow (low velocity relative to the tumbler wall), while the darker gray particles are in the flowing layer. At the outset of the simulations, we “tag” a vertical line of particles within the flowing layer and denote their original orientation with a black arrow (see frames (a) and (d)). In the other frames, the green arrows denote the future average position and orientation of the initially tagged particles as they move through the bed. The broken, red arrow in frame (f) represents a particle orientation that has “folded” upon itself (i.e., the orientation contains a loop from a partial layer pass). Note that the orientation of the arrow in the unbaffled case both leaves and enters the flowing layer almost perfectly tangent, while the orientation of the arrow in the baffled case is rotated roughly  $90^\circ$ . The plot on the right shows the distribution of rotations between particle layer passes for various tumbler configurations. The black symbols represent the unbaffled case and a case with (short) traditional baffles, both of which have very narrow distributions centered on 0.5 rotations. In contrast the axially located baffles (green and blue symbols) or long traditional baffles (red symbols) result in much broader distributions, suggesting that the orientation of particles in future layer passes should be almost uncorrelated with previous passes. Note that we define long traditional baffles as those that actually transversely cut a portion of the flowing layer, much like the axially oriented baffles.

gation with respect to the tumbler streamlines (as the baffles rotate with the drum; see Fig. 3). This leads to results quite similar to those seen in the zigzag mixer as the static bed no longer returns the material to the flowing layer(s) in the same orientation in which it left. Another way to analyze the flow is shown in the plot at the right of Fig. 3. Recalling that a single pass through the shearing layer would reorient particles by  $180^\circ$ , one notes that the segregation orientation will change during the mixing process if the particles pass through the layer, on average, in fewer than one half of a rotation. The number of rotations per layer pass is almost exactly 0.5 for an unbaffled mixer, and one with (shorter) traditional baffles; however, the distribution of rotation times broadens considerably both for long traditional baffles and for any number of axial baffles.

Figure 4 depicts qualitative images and Fig. 5 shows quantitative measures of the asymptotic mixing for both experiments and simulations, for both bidisperse density and size-related segregation. Both the DEM simulations

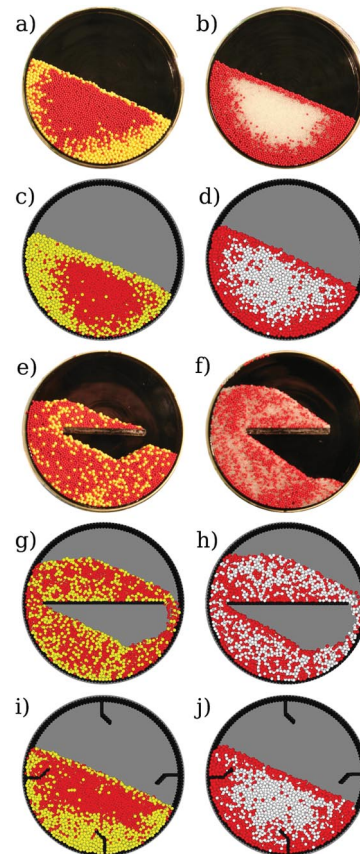


FIG. 4 (color). Asymptotic mixing results in tumbler mixers for both size (left) and density (right) segregation. Unbaffled tumblers [(a) and (b), experiments; (c) and (d), simulations] result in strong radial segregation. In contrast, baffles that truncate the flowing layer [shown experimentally in (e) and (f), and computationally in (g) and (h)] dramatically reduce the degree of segregation. For comparison, computational results for a traditional baffle arrangement are shown in (i) and (j).



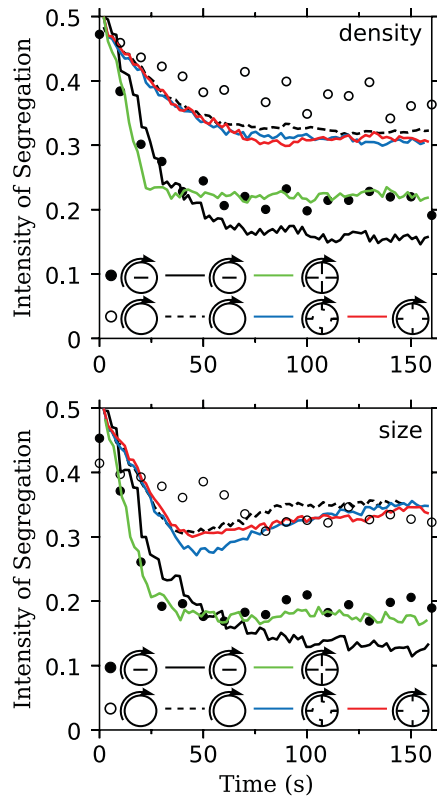


FIG. 5 (color). Quantitative mixing results in tumbler mixers for both density (top) and size (bottom) segregation. Experiments are shown as symbols and simulations as lines. Note that unbaffled mixers and mixers with short baffles behave very similarly, while axial baffles or very long traditional baffles results in significantly lower IS values (increase the degree of mixing).

and the experiments use 1.5–4 mm glass and acetate particles in short (6 particle diameters) 70 particle wide tumblers which are rotated at 6 RPMs. Size segregation involves a 3:2 ratio (3 mm:2 mm), while density segregation involves a 2:1 ratio (glass:acetate). The simulated particle sizes and densities (as well as vessel size) are matched to their corresponding experiments, the particle stiffness used is reduced in order to decrease necessary simulation time (a practice shown to have essentially no impact on flow kinematics [29]). While the (short) traditional baffles produce results similar to the nonbaffled case, axially located baffles dramatically reduce the measured asymptotic degree of segregation as do the very long traditional baffles.

While we have demonstrated two simple examples of flow modulation, the method described here is entirely general. As long as the flow perturbations alter the direction of segregation (relative to the previous particle flow history) at high enough frequencies, this technique may be used for a wide range of particle processing applications, ranging from mixing to conveying, and can have a significant impact in industries from foodstuffs to ceramics to pharmaceuticals.

This work was supported by the Chemical and Transport Systems Division of the National Science Foundation (Grant No. 0331352 and No. 0553763).

\*jjmcc@pitt.edu

- [1] R.L. Brown, *Inst. Fuel* **10**, 15 (1939).
- [2] J.C. Williams, *Powder Technol.* **15**, 245 (1976).
- [3] T. Mullin, *Science* **295**, 1851 (2002).
- [4] J. Ottino and D. Khakhar, *Annu. Rev. Fluid Mech.* **32**, 55 (2000).
- [5] S. Conway, T. Shinbrot, and B. Glasser, *Nature (London)* **431**, 433 (2004).
- [6] K.M. Hill, D.V. Khakhar, J.F. Gilchrist, J.J. McCarthy, and J.M. Ottino, *Proc. Natl. Acad. Sci. U.S.A.* **96**, 11 701 (1999).
- [7] H.A. Makse, S. Havlin, P.R. King, and H.E. Stanley, *Nature (London)* **386**, 379 (1997).
- [8] O. Pouliquen, J. Delour, and S.B. Savage, *Nature (London)* **386**, 816 (1997).
- [9] D.V. Khakhar, J.J. McCarthy, and J.M. Ottino, *Phys. Fluids* **9**, 3600 (1997).
- [10] J.B. Knight, H.M. Jaeger, and S.R. Nagel, *Phys. Rev. Lett.* **70**, 3728 (1993).
- [11] N. Burtally, P. King, and M. Swift, *Science* **295**, 1877 (2002).
- [12] H. Li and J. McCarthy, *Phys. Rev. Lett.* **90**, 184301 (2003).
- [13] A. Samadani and A. Kudrolli, *Phys. Rev. Lett.* **85**, 5102 (2000).
- [14] N. Jain, J.M. Ottino, and R.M. Lueptow, *Phys. Rev. E* **71**, 051301 (2005).
- [15] G. Félix and N. Thomas, *Phys. Rev. E* **70**, 051307 (2004).
- [16] S.B. Savage and C.K.K. Lun, *J. Fluid Mech.* **189**, 311 (1988).
- [17] J.T. Jenkins and S.B. Savage, *J. Fluid Mech.* **130**, 187 (1983).
- [18] C.S. Campbell, *Annu. Rev. Fluid Mech.* **22**, 57 (1990).
- [19] J.M. Ottino, *The Kinematics of Mixing: Stretching, Chaos, and Transport* (Cambridge University Press, New York, 1989).
- [20] J.J. McCarthy, T. Shinbrot, G. Metcalfe, J.E. Wolf, and J.M. Ottino, *AIChE J.* **42**, 3351 (1996).
- [21] C. Wightman, P.R. Mort, F.J. Muzzio, R.E. Riman, and R.K. Gleason, *Powder Technol.* **84**, 231 (1995).
- [22] S.J. Fiedor and J. Ottino, *J. Fluid Mech.* **533**, 223 (2005).
- [23] D.V. Khakhar, J.J. McCarthy, and J.M. Ottino, *Chaos* **9**, 594 (1999).
- [24] S.B. Savage, in *Disorder and Granular Media*, edited by D. Bideau and A. Hansen (Elsevier Science, Amsterdam, 1993), p. 255.
- [25] P.A. Cundall and O.D.L. Strack, *Géotechnique* **29**, 47 (1979).
- [26] H.A. Makse and J. Kurchan, *Nature (London)* **415**, 614 (2002).
- [27] S.T. Nase, W.L. Vargas, A.A. Abatan, and J.J. McCarthy, *Powder Technol.* **116**, 214 (2001).
- [28] D.V. Khakhar, J.J. McCarthy, T. Shinbrot, and J.M. Ottino, *Phys. Fluids* **9**, 31 (1997).
- [29] O. Walton, *Int. J. Eng. Sci.* **22**, 1097 (1984).